Journal of Wind Engineering & Industrial Aerodynamics 242 (2023) 105588

Contents lists available at ScienceDirect

Journal of Wind Engineering & Industrial Aerodynamics

journal homepage: www.elsevier.com/locate/jweia

Effects of different aerodynamic configurations on crosswind stability of a conventional train

Carlos Esteban Araya Reyes [a,*], Daniele Rocchi [a], Gisella Tomasini [a], Mikel Iraeta Sánchez [b], Maialen Artano [b]

[a] Politecnico di Milano, Milan, Italy
[b] Construcciones y Auxiliar de Ferrocarriles, Beasain, Spain

ARTICLE INFO

Keywords:
Conventional train aerodynamics
Crosswind
CWC
Wind tunnel
Roof and underbody aerodynamics

ABSTRACT

Crosswind stability studies have been multiplied since the 90s due to the increase in speed and the continuous weight reduction of the railway vehicles. At beginning, most of the attention was devoted to high-speed trains but recent studies have shown also conventional trains that runs at considerably lower speeds may also have a high risk of overturning due to crosswind. In this study, a conventional train designed by CAF has been analysed to evaluate the impact that different roof and underbodies have on the aerodynamic performance of the train. In the Wind Tunnel of Politecnico di Milano, a modular scaled model was tested to determine the aerodynamic coefficients of the different train configurations. Moreover, the procedure described in the European Standard EN14067-6 to assess train stability under crosswind was applied to evaluate the Characteristic Wind Curve (CWC) using time-dependent multibody simulations and the 'Chinese hat' wind time history for each train composition. Results have shown a significant improvement is obtained for some configurations, especially when the roof is closed covering the roof equipment with an increment of around 4 m/s on characteristic wind speed.

1. Introduction

Since the 1980s and 1990s, given the increase in high-speed trains, ever faster and lighter, studies for the evaluation of the risk of overturning due to crosswind have multiplied (Araya Reyes et al., 2023a; Baker, 1991a, 1991b, 1991c; Bocciolone et al., 2008; Hemida and Krajnović, 2009; Liu et al., 2020; Tomasini and Cheli, 2013) and have led to the definition of complete regulations (EN14067-6, 2018; TSI, 2014), for the characterisation and homologation of new high-speed trains, it means, trains with top speeds exceeding 250 km/h.

As part of the aerodynamic characterisation of the vehicle against crosswinds, Characteristic Wind Curves (CWC) must be determined. The CWCs represent the wind speed a vehicle is able to withstand as a function of train speed and wind angle in some reference conditions. Thus, they do not represent the limits for the overturning of the vehicle in operational conditions but give a common reference frame to compare different vehicles.

More recently, however, new studies on conventional trains (having maximum speeds ranged between 160 km/h and 250 km/h) have highlighted that the characteristic wind speeds found for those vehicles are not turn out to be significantly higher (and therefore less critical) than those found for high-speed trains (Araya Reyes et al., 2022, 2023b; Giappino et al., 2016; Paradot et al., 2015). And it has been highlighted the necessity of more research on this topic (Diedrichs, 2010; Villalmanzo Resusta et al., 2018).

Considering that, at national level, only UK, Germany and France have National Standards on this item also for trains having a top speed lower than 250 km/h, new International Projects, as AeroTRAIN (RSSB, 2013) and SAFIRST (UIC, 2021a, 2021b; 2021c), launched in 2019 b y UIC and still ongoing, have been funded by European Union with the goal of reaching common rules also for these trains.

Some studies have been made on the influence that different parts of the vehicle have on the general performance of a train under crosswind, for example nose shape, roof curvature, bogie geometry or inter-car gap dimensions (Chen et al., 2018; Guo et al., 2020; Hemida and Krajnović, 2010; Liu et al., 2022; Muñoz-Paniagua and García, 2019; Sicot et al., 2018; Xia et al., 2021; Zhang et al., 2018). Others are focused on optimising the shape of high-speed trains to improve the behaviour under crosswind with special attention in nose shape (Cheli et al., 2010; Shuanbao et al., 2014; Wang et al., 2021). But, while high-speed trains

* Corresponding author.
E-mail address: carlosesteban.araya@polimi.it (C.E. Araya Reyes).

https://doi.org/10.1016/j.jweia.2023.105588
Received 22 May 2023; Received in revised form 18 October 2023; Accepted 18 October 2023

are characterised by different noses but similar car-body shapes, conventional trains present a larger variety of aerodynamic characteristics and lend themselves better to an aerodynamic optimisation aimed at minimising the risk of overturning associated to crosswind. Moreover, the effect of other sections of the carbody, for example, the effects of having a fully covered roof or one with exposed equipment, or different underbody geometries, have not been widely studied, especially for conventional trains.

For all these reasons, the present study has the objective to evaluate how different configurations of roofs and underbodies of first and second vehicle of a conventional train have an impact on the safety to crosswind.

A train designed by the company CAF (Construcciones y Auxiliar de Ferrocarriles S.A.) characterised by a top speed of 200 km/h has been considered for this study; as prescribed by the homologation procedure for high-speed trains contained in (TSI, 2014) and the (EN14067-6, 2018), the aerodynamic coefficients of the first two cars, in different configurations, have been experimentally measured by wind tunnel tests on scale models.

Finally, the corresponding CWCs have been numerically evaluated by multi-body simulations using, as wind model, the ideal deterministic wind speed time history named 'Chinese Hat'.

In the next section an overview of the studied train and configurations analysed as well as the methodology adopted are presented; section 3 describes the wind tunnel tests in terms of experimental setup and measured force aerodynamic coefficients while section 4 is about the numerical evaluation of the corresponding CWCs.

2. Description of the studied train and methodology

The model of the studied train was designed by the company CAF and based on a conventional train (see Fig. 1) with a maximum speed of 200 km/h. The train composition is formed by 10 cars with shared (Jacob) bogies and standard gauge. For the wind tunnel test a reduced 3 car composition has been studied. The main dimensions of the train are summarised in Table 1.

For the scope of the study, 11 configurations, characterised by different roofs and underbodies, are considered. The baseline configuration corresponds to configuration A. In configurations B, C, D, E and F only the first car of the train is changed while the second remains unchanged: configurations A, B and C differ only in the roof of the first vehicle. Configuration D differs from the baseline configuration in the underbody of the first car. Configurations C, E and F have the same covered roof but different underbody configurations.

In configurations G, H, I, J and K the first coach is set in baseline configuration, while only the second car is modified: configuration G, and H differs from A only on the roof of the second car, G has the HVAC covers while in H the roof is completely covered. Configuration I and J are analogous to configurations A and H but with the empty underbody.

Table 1
Train main dimensions.

	First Car	Intermediate Car
Body length	22.45 m	17.00 m
Body height	4.23 m	4.06 m

Configuration K has a slightly different roof configuration compared with A, and an underbody design without fenders.

The analysed train configurations are depicted in Fig. 2, and summarised in Table 2.

2.1. Methodology

To evaluate the effects that the different configurations have on the stability of the studied train, the procedure described in the European Standard is followed.

The reference standard for assessing railway stability under crosswinds corresponds to EN14067-6 - Requirements and test procedures for cross wind assessment (EN14067-6, 2018). The standard is applicable to all passenger vehicles, locomotives, and power cars with a maximum train speed above 140 km/h up to 360 km/h. But only for vehicles with a maximum train speed between 250 km/h and 360 km/h, a requirement to demonstrate the crosswind stability is imposed by the reference CWCs.

Two methodologies are applicable for vehicles on this speed range: a simplified proof which is more conservative (commonly used for preliminary design stage calculations) but not applicable for articulated trains and a full proof of crosswind stability (commonly used for full homologation purposes).

In this work, the full proof of stability using time-dependent multibody simulations is applied: according to this procedure, the wheel loads are obtained as a response of the dynamic vehicle model to the 'Chinese hat' wind scenario.

For the full proof of crosswind stability, the aerodynamic characterisation of the studied geometry is performed by means of the aerodynamic coefficients that shall be obtained by wind tunnel tests on scaled models.

3. Wind tunnel tests

The first part of the analysis consists in the evaluation of the aerodynamic coefficients of all the analysed configurations. The experimental campaign is performed at the Wind Tunnel of Politecnico di Milano. This facility is composed by a closed-circuit wind tunnel with two test sections disposed in vertical configuration (Fig. 3). In the upper level is placed the low-speed boundary layer test section with a cross section of 13.84 m × 3.84 m. While the high-speed low turbulence test section of 4 m × 3.84 m is placed in the lower part of the circuit. The

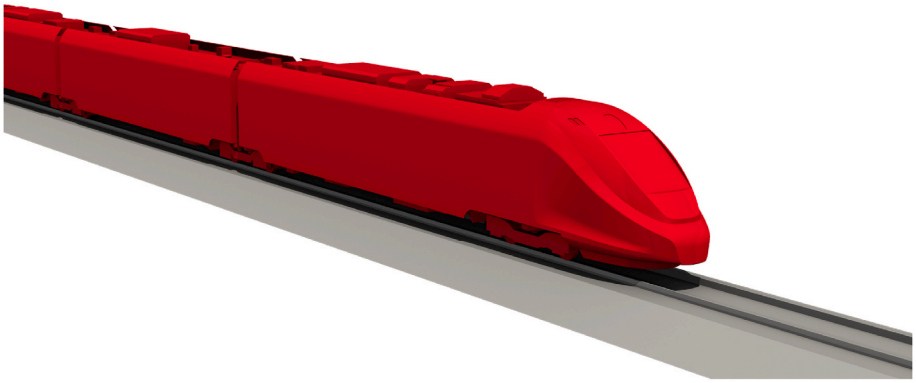

Fig. 1. Conventional train designed by CAF.

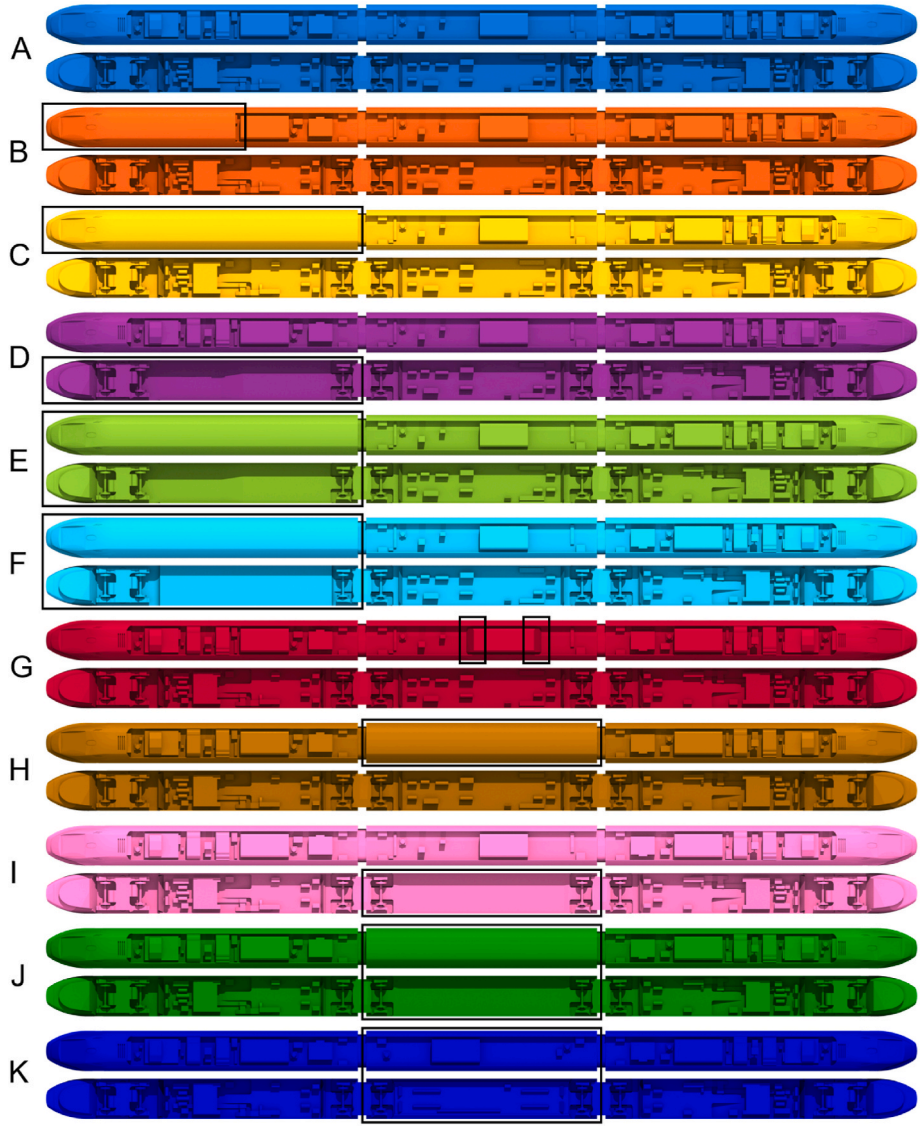

Fig. 2. Train configurations. Upper and bottom view of the 11 configurations analysed.

Table 2
Summary of train configurations analysed.

Configuration	First Car		Second Car		Third Car
	Roof	Underbody	Roof	Underbody	
A	Baseline	Baseline	Baseline	Baseline	Dummy
B	Half covered	Baseline	Baseline	Baseline	Dummy
C	Covered	Baseline	Baseline	Baseline	Dummy
D	Baseline	Smooth	Baseline	Baseline	Dummy
E	Covered	Smooth	Baseline	Baseline	Dummy
F	Covered	Covered	Baseline	Baseline	Dummy
G	Baseline	Baseline	HVAC fenders	Baseline	Dummy
H	Baseline	Baseline	Covered	Baseline	Dummy
I	Baseline	Baseline	Baseline	Smooth	Dummy
J	Baseline	Baseline	Covered	Smooth	Dummy
K	Baseline	Baseline	Open	45° Fender	Dummy

overall characteristics of the wind tunnel are summarised in Table 3.

The series of tests to study the performance of the train in its different configurations are carried out at the high-speed low turbulence section, characterised by a maximum speed of 55 m/s and a turbulence intensity lower than 0.15%.

3.1. Experimental setup

The experimental setup used during the test consists in a three-car convoy set on a Single-Track Ballast and Rails (STBR), in compliance with the European Standard (EN14067-6, 2018) mounted over a splitter plate to guarantee the correct wind profile.

The train model is scaled by the ratio 1:20.6 to fulfil the standard requirement on the ratio convoy length over wind tunnel width (that shall be lower than 0.75) with a model composed by three full cars. The tested train set is represented in Fig. 4 and is composed by.

- the first car, instrumented;
- the second car, instrumented;
- the down-stream dummy vehicle (whose geometry coincides with the first/last car), fixed to the ground and placed next to the second vehicle as boundary condition (full vehicle).

The correct separation between adjacent vehicles is replicated. Mechanical contact between vehicles is always avoided by leaving the corresponding inter-car gap. The simplified geometries of the vehicles, including bogies, are built exactly as designed in the reference CAD model proportioned by CAF. The shared bogie is divided into two pieces,

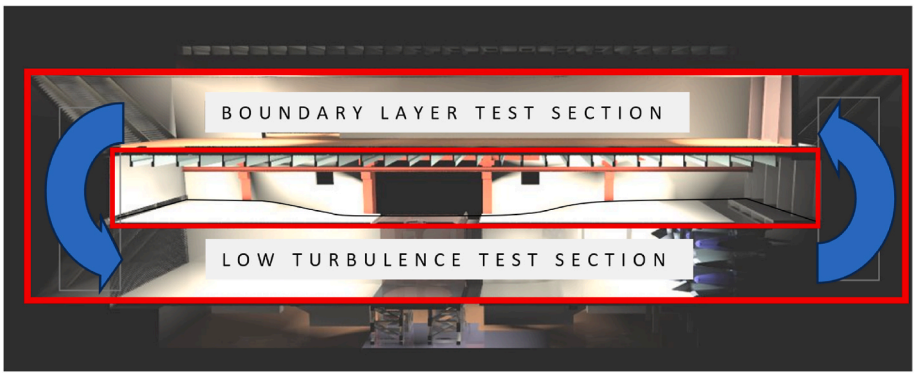

Fig. 3. Wind Tunnel longitudinal cross section.

Table 3
Overall Politecnico di Milano Wind Tunnel characteristics.

Tunnel Overall Dimensions			50 × 15 × 15 (m)	
Maximum Power (Fans only)			1.5 (MW)	
Test Section	Size [m × m]	Max Speed [m/s]	$\Delta U/U$ [-]	Turb. Int. I_u%
Boundary Layer	13.84 × 3.84	16	< ± 3	<1.5
Low Turbulence	4 × 3.84	55	< ± 0.2	<0.15

each one connected to one of the wagons as can be seen in Figs. 5 and 6.

The scaled model is built in a modular way to avoid manufacturing a separate model to represent each tested configuration and reduce the time spent changing configurations. As it can be seen from Fig. 7, first and second vehicles are composed by three parts.

- the main body, rigidly attached to the dynamometric balance;
- interchangeable underbody, bolted to the main body;
- interchangeable roof, bolted to the main body.

In order to measure the aerodynamic loads, each one of the first two cars are instrumented with a 6-components dynamometric balance. The balance used for the test corresponds to the RUAG Aerospace model 192 strain-gauge based balance, that is mounted inside the model as shown in Fig. 8.

The wind tunnel tests are performed at the nominal wind speed of V = 50 m/s. The duration of every test is 20 s.

The corresponding Reynolds number obtained from equation (1):

$$Re = \frac{V * D}{\nu} \tag{1}$$

where the characteristic dimension D is the reference length (D = 3 m at real scale) while ν is the air kinematic viscosity ($\nu = 1.5 \times 10^{-5}$ [m^2/s]). With the nominal wind speed, the Reynolds number is equal to $Re_{max} = 4.9 \times 10^5$, that satisfies the European Standard requirement ($Re > 2.5 \times 10^5$, see section 5.3.4.5 of (EN14067-6, 2018)).

3.2. Analysis of results

The results obtained from the wind tunnel tests made for the first two cars of the train in different aerodynamic configurations are represented in terms of force and moment coefficients defined with equations (2) and

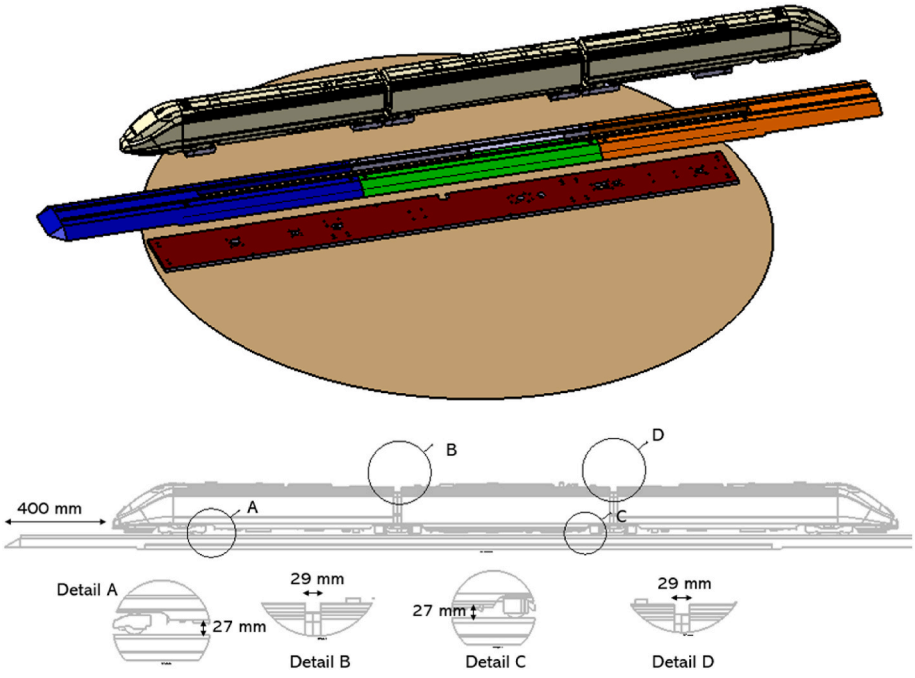

Fig. 4. Setup of the analysed train for wind tunnel tests.

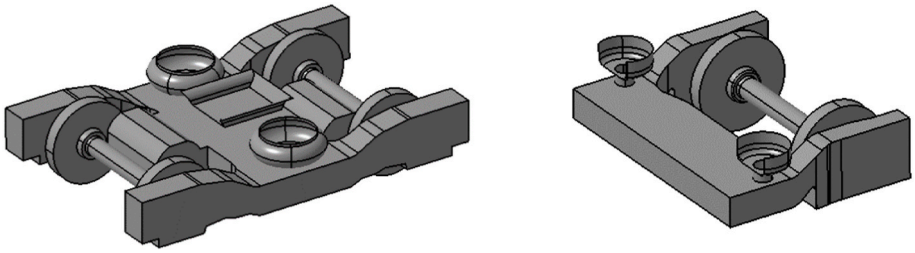

Fig. 5. CAD model of the bogie. Left: Complete bogie. Right: Half model.

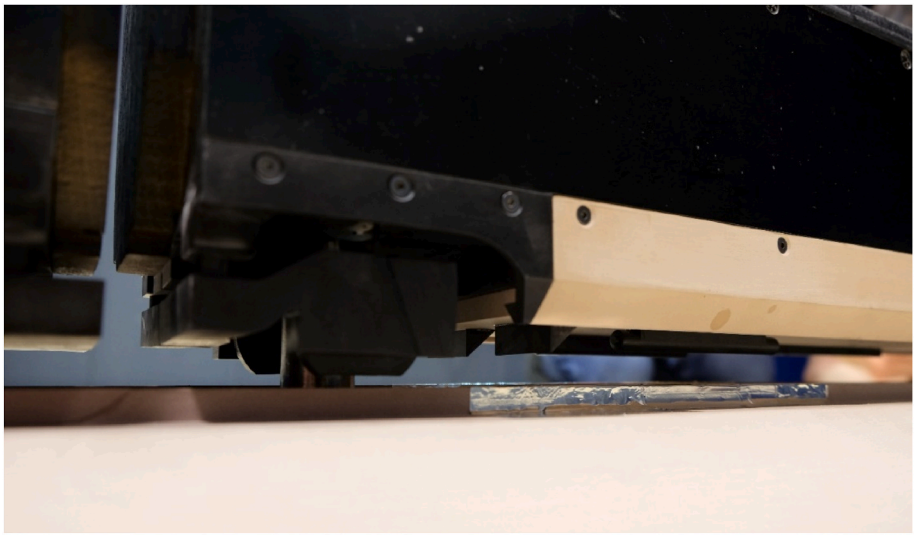

Fig. 6. Picture of half bogie model.

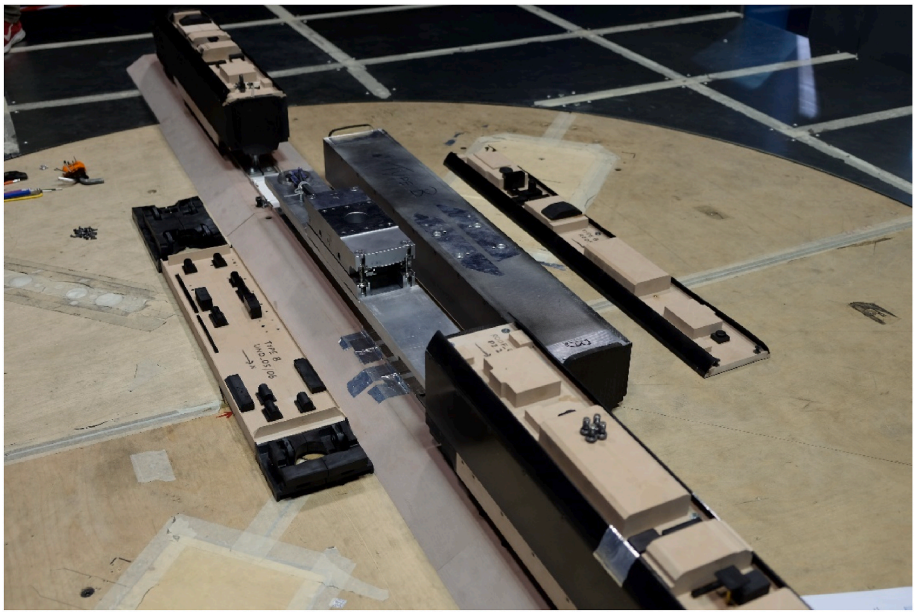

Fig. 7. Disassembled wind tunnel model. The balance is mounted on the rigid support fixed to the splitter plate, and the car body is composed by the interchangeable roof and underbody mounted on the main body.

(3) as defined in (EN14067-6, 2018).

$$C_{Fi} = \frac{2F_i}{\rho v^2 A_0}, i = x, y, z \tag{2}$$

$$C_{Mi} = \frac{2M_i}{\rho v^2 A_0 d_0}, i = x, y, z \tag{3}$$

Where $A_0 = 10$ m^2 and $d_0 = 3$ m are the reference normalisation area

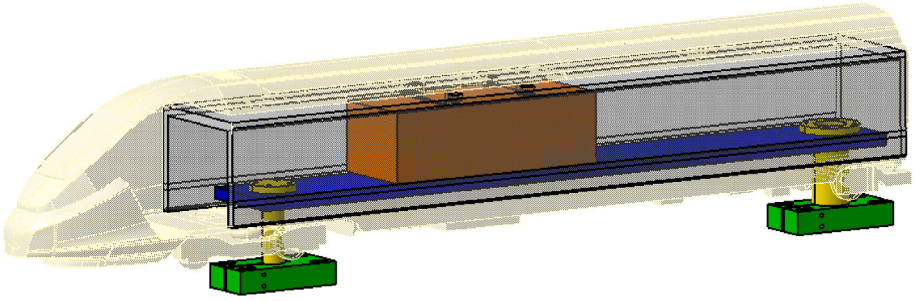

Fig. 8. Internal structure that supports the balance for the wind tunnel tests.

and length respectively.

The normalisation is obtained by dividing each coefficient by the $C_{Mx,lee}$ value at 90° of the base configuration (configuration A in Table 1), according to the following equation (4):

$$C_{i,n} = \frac{C_i}{C_{Mx,lee;@90^\circ}}, i = F_x, F_y, F_z, M_x, M_{x,lee} \quad (4)$$

The results for the first three configurations, in which only the roof of the first vehicle is changed are presented in Fig. 9. It can be observed that up to 30° yaw angle, the values of all coefficients are very similar. This behaviour can be attributed to the fact that development of the flow at lower angles is dictated mostly by the shape of the nose. At greater angles the effect of the roof becomes more important.

In the case of C_{Fy} and C_{Mx} the main differences can be observed in the range from 30° to 70°. It is possible to observe that the configuration with the partially or fully closed roof, B and C respectively, show lower aerodynamic coefficients. Previous CFD experience on conventional train geometries suggests the reduction in lateral force may be explained by the differences in the airflow generated at the leeward side of the car body. When the flow remains attached to the roof the vortex structures generated are probably smaller and less strong. At yaw angles above 70°, the behaviour corresponds to that of a bluff body, the vortex travelling parallel to the train is not present anymore, explaining why all the three roof configurations give equivalent results.

The differences appreciated for the vertical force coefficient show the expected trend. Configuration C, with the roof fully covered, is the one with higher values of lift, followed by the configuration B, with half of the roof covered, and the lowest values are found for configuration A. The attached and accelerated flow over the roof produces more lift. Therefore, the bigger the section covered, the bigger is the lift generated.

In the configurations C, E and F the completely covered roof is kept fixed, while the underbody is changed. The results are reported in Fig. 10. It can be seen that the underbody has a very small effect on coefficients. Configurations C and E have almost equal results even if the underbody in C configuration is characterised by the presence of a lot of equipment: this behaviour may be explained considering that the flow separation is induced at the edge of the lateral fender, and the equipment is efficiently covered. In the case of configuration F, the flow seems to remain attached to the underbody, reducing the lift generated by the vehicle. From the results it can be observed that an underbody with a well-designed lateral fender and an underbody completely covered may have a similar performance.

Similar considerations can be obtained when comparing configuration A and configuration D (Fig. 11). In this case, the open roof is the same in both configurations while the underbody is changed: in configuration A the underbody presents a lot of equipment while in D it is smooth but with the same lateral fenders. The results show that the effect of the underbody equipment is almost negligible, obtaining a very small variation in the results for the two configurations. It can be noted a little increment in coefficients in the range from 30° to 70° when the empty underbody is used, which is consistent with the results obtained for configuration C and E.

Fig. 12 presents the results of all the six configurations of the first vehicle: it is possible to conclude that the most favourable

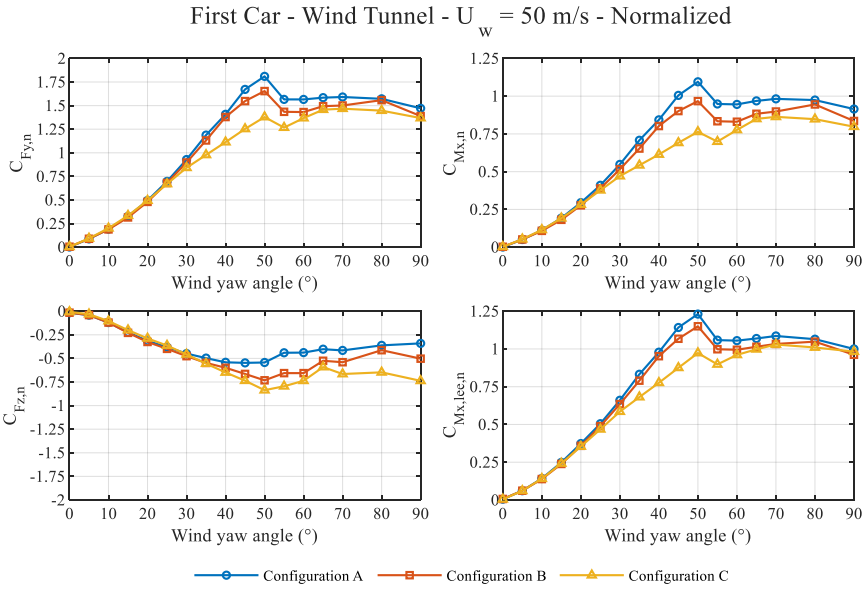

Fig. 9. Wind tunnel tests, first car, U_w = 50 m/s: comparison between normalised aerodynamic coefficients measured on configurations A, B and C.

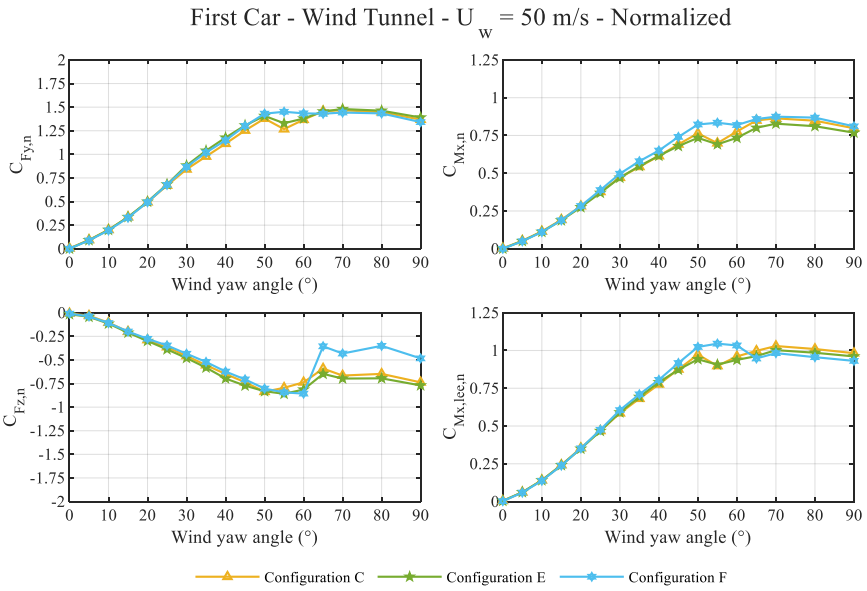

Fig. 10. Wind tunnel tests, first car, $U_w = 50$ m/s: comparison between normalised aerodynamic coefficients measured on configurations C, E and F.

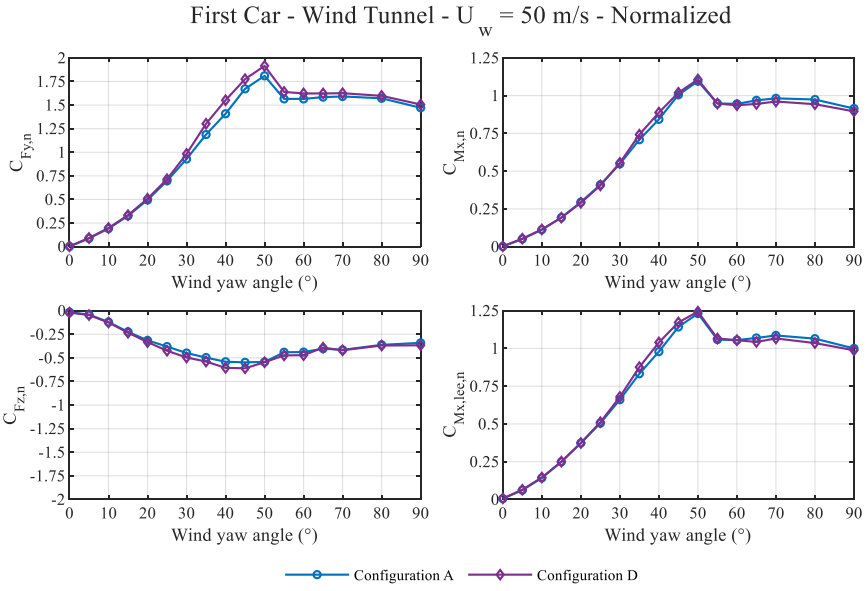

Fig. 11. Wind tunnel tests, first car, $U_w = 50$ m/s: comparison between normalised aerodynamic coefficients measured on configurations A and D.

configurations are the ones with open underbody and closed roof.

For the second car of the train, the results for configurations A, G and H, in which the underbody is kept unchanged while the roof varies are reported in Fig. 13. The effect of HVAC fenders (configuration G) is almost negligible because the system is already covered by the lateral fenders of the roof. Anyway, some beneficial effects can be observed in the range of wind yaw angle from 30° to 50° for lateral force and roll moment coefficients, while for the lift coefficient a detrimental effect is observed. The combination of these two effects gives an almost unchanged trend of the lee-rail rolling moment with respect to configuration without HVAC fenders.

On the other hand, when the second car with the roof completely covered (configuration H) is compared with the baseline configuration, a huge difference can be observed. There is a big reduction in lateral force and roll moment, but there is also an important increment in lift force coefficient from 30° onwards. Despite the lift increment, the closed roof leads to a big improvement when compared to the base design: this can be observed from the resultant roll moment with respect to the lee rail ($C_{Mx,lee}$) where a clear reduction is observed at almost all yaw angles except 90°.

In Fig. 14, the coefficients for configurations A, H I and J are shown, and the effect of the roof can be confirmed. From the results plotted, two branches of curves can be clearly appreciated from 30°: the two configurations with closed roof (H, J) show lateral force and both moment coefficients significantly lower, when compared to the ones with open roof. On the other hand, the effect of the underbody is lower but consistent: in both cases, the smooth underbody leads to a further reduction in the lee-rail rolling coefficient $M_{x,lee}$ from 30° onwards.

Results for all the six configurations regarding the second car are plotted in Fig. 15. Configuration K, with open roof but with less

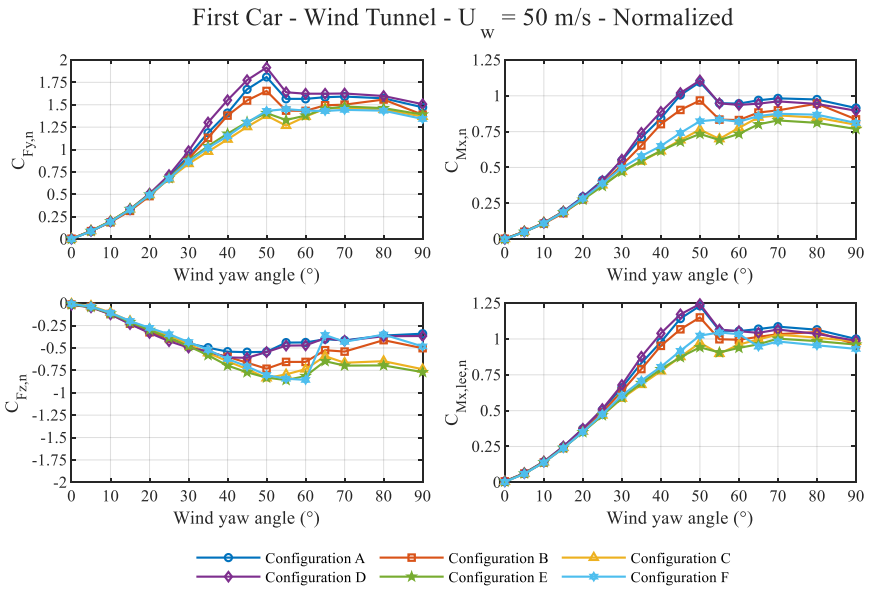

Fig. 12. Wind tunnel tests, first car, $U_w = 50$ m/s: comparison between normalised aerodynamic coefficients measured on configurations A to F.

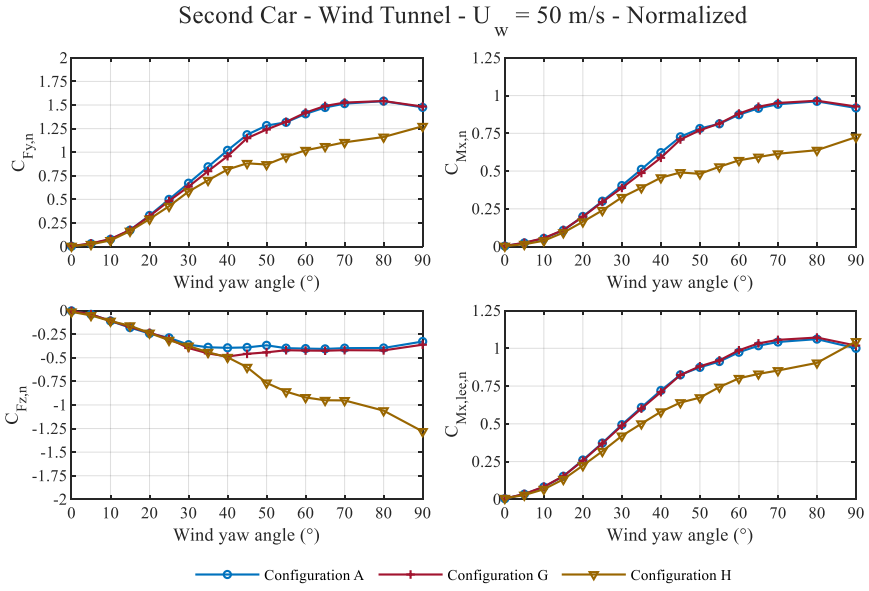

Fig. 13. Wind tunnel tests, second car, $U_w = 50$ m/s: comparison between normalised aerodynamic coefficients measured on configurations A, G and H.

equipment over it than configuration A, and with a different design of the underbody, shows a behaviour in line with the other open roof designs. Compared with baseline, the design of the underbody in K configuration has a detrimental effect, as expected, due to the fenderless design leaving the equipment more exposed.

4. Effects on vehicle stability

To evaluate the final effect on cross wind stability of the different configurations analysed in the previous section, a crosswind stability assessment is performed according to the methodology described in (EN14067-6, 2018). To assess the stability of the train, the methodology requires the determination of the 'characteristic wind speed', defined as the maximum wind speed with a given yaw angle that a train running at certain speed can withstand before the wheel unloading threshold is exceeded. The collection of characteristic wind speeds for a varying parameter (in this work for varying train speed) is called Characteristic Wind Curve (CWC).

4.1. CWC procedure description

For the full proof of crosswind stability, the standard proposes two methods to assess the vehicle response to the wind action and determine the wheel unloading. One method involves the application of an advanced quasi-static approach, simpler and more conservative; whereas the other option requires time-dependent multi-body simulations where wheel loads are obtained from the response of the vehicle model to the 'Chinese hat' wind scenario applied. In this study the second approach is used.

From the 'Chinese hat' wind scenario, wind forces are computed according to section 5.4.4.2 of (EN14067-6, 2018). The resultant aerodynamic loads to be applied as an input to the vehicle model $F_{wind}(t) =$

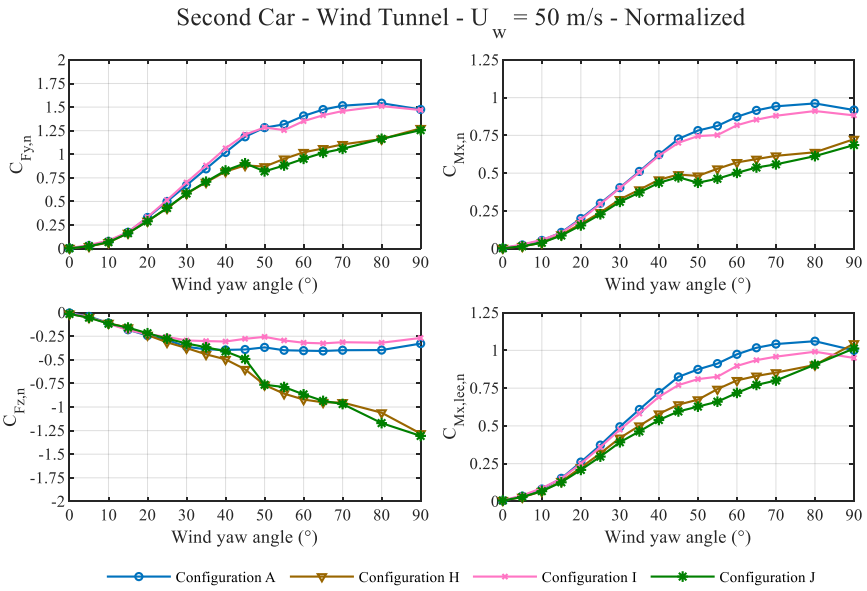

Fig. 14. Wind tunnel tests, second car, $U_w = 50$ m/s: comparison between normalised aerodynamic coefficients measured on configurations A, H, I and J.

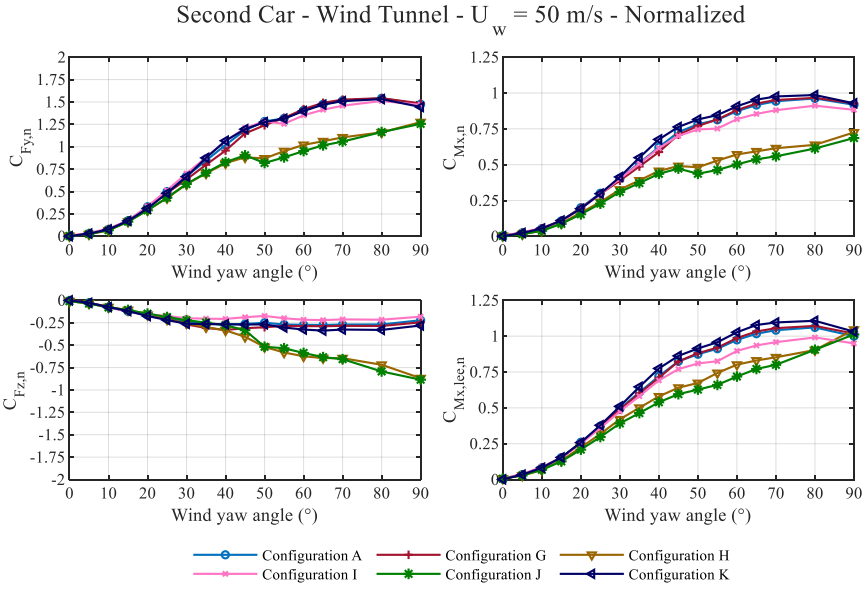

Fig. 15. Wind tunnel tests, second car, $U_w = 50$ m/s: comparison between normalised aerodynamic coefficients measured on configurations A and G to K.

$\{F_i, M_i\}$ depend on the aerodynamic coefficients, train speed, wind speed and yaw angle. Thus, an iterative process is carried out where the vehicle response (and thus, wheel unloading) is calculated for different combinations of train speed and wind speed.

From the results of the multibody simulations, the wheel unloading criterion is evaluated to determine the CWC. According to (EN14067-6, 2018) a wheel unloading of 90% will define the CWCs. The wheel unloading is defined by equation (5), where ΔQ is the average vertical force variation of the most critical bogie and Q_0 is the average static vertical wheel load on the most critical bogie.

$$\frac{\Delta Q}{Q_0} < 0.9 \tag{5}$$

The full proof of stability using time-dependent multi-body simulations can be summarised as follows.

1. Determination of the wind time history based on the 'Chinese hat' model.
2. Determination of the relative wind speed and yaw angle.
3. Calculation of aerodynamic loads to be applied to the multi-body model considering the relative wind speed and yaw angle.
4. Computation of the dynamic response of the vehicle subjected to the wind loads using multi-body simulations.
5. Evaluation of the wheel unloading criteria to obtain the Characteristic Wind Speed.
6. Repeat for different train speeds.

The set of Characteristic Wind Speeds computed for different winds speed corresponds to the CWC.

4.2. Multi-body model description

Multibody simulations are performed by SIDIVE code, a multibody dynamics simulation tool developed in-house by CAF.

Bodies are modelled through their inertial (and possibly elastic) properties, while linkages are described by geometric constraints. The behaviour of the complete multibody system is governed by the set of equations of motion. Given the initial conditions and applied loads, the solution of those equations provides the temporal evolution of the degrees of freedom of the system and thus the motion of each body.

The different parts of the train model in SIDIVE include: wheelsets, bogies and car bodies. Due to their high stiffness and thus high natural frequencies (well beyond the running dynamics range of interest), wheelsets are usually considered as rigid bodies with 6 degrees of freedom, i.e. longitudinal, lateral and vertical displacement, as well as the rotation around each of these axes. On the contrary, the flexibility of bogies and car body is accounted by means of their dominant vibration eigenmodes, obtained from finite element analysis, since they are critical for an accurate assessment of safety and comfort.

Suspension elements are modelled by means of springs, dampers, friction and bump stops, as well as applicable kinematic constraints. When pertinent, the nonlinear characteristics of such elements are modelled; that is, the real force/displacement and force/speed curves are considered.

Wheel-rail interaction in SIDIVE is based on elastic contact, that is, the material flexibility is taken into account: both the wheel and the rail deform locally according to the forces they are subjected to (and the corresponding constitutive laws). By default, standard railway steel properties are assumed.

An in-house plugin for SIDIVE is used for the determination and application of the aerodynamic loads as a consequence of the wind action on the vehicle model. The plugin drives a series of multibody simulations that yield the CWCs for the defined train speed, wind speed, wind angle, and non-compensated lateral acceleration value.

The following input data shall be provided to the plugin for the simulation process.

- Case file: A reference file where the considered simulation cases are defined.
  - o As previously stated, simulations will be carried out for a different combination of train speed/wind speed.
  - o Additionally, this process may be repeated for different non-compensated acceleration values.
- Aerodynamic coefficients for each car of the vehicle model.
- Ground configuration: in this case, STBR ground configuration has been used according to (EN14067-6, 2018).
- The vehicle dynamic model defined using SIDIVE.

The output of each simulation case will be the wheel unloading ΔQ for each bogie of the vehicle model. Once the simulation process is completed the plugin will use all the obtained results to determine the CWCs defined by the 90% wheel unloading of the most critical bogie (the process is summarised in the flow chart displayed in Fig. 16).

4.3. Analysis of results

In Fig. 17, the CWCs computed at 90° for the six configurations considered for the first car of the train are reported. As expected from the behaviour of the aerodynamic coefficients, two branches can be clearly observed. Configurations C, E and F, corresponding to the closed roof designs, present the best results, with higher values of characteristic wind curves. An interesting consideration is that the result for the half-covered roof (configuration B) is much closer to the case with open roof at lower speeds (under 160 km/h). As the train speed increases, due to the reduction in resultant wind yaw angle, the performance of the half-covered roof gets closer to the fully covered roof configurations.

The major differences can be noticed in the range from 90 to 170 km/h which corresponds to common range of operation of conventional trains: in this range an improvement of around 10% is observed. In fact, at 100 km/h a difference of more than 13%, which is equivalent to an increment of more than 4 m/s in characteristic wind speed, is found between the baseline configuration and configuration E with closed roof.

Considering that at the moment there is no reference CWC in the European Standards for conventional trains, in order to put into perspective the significance of these results, it is possible to consider the extended reference CWC for high-speed trains (EN14067-6, 2018). The reference characteristic wind speed for a high-speed train at 100 km/h, with the wind blowing at 90° is 33.8 m/s, the same value obtained for the base configuration (configuration A). Therefore, the increment of 4 m/s obtained with the closed roof and smooth underbody (configuration E) brings the train to a much favourable situation in terms of crosswind stability. For the studied train, the practical implications of the improved design with the correspondent increment of 4 m/s of characteristic wind speed are multiple. From the point of view of vehicle design, more freedom is given to the manufacturer, allowing for example a further weight reduction with the consequent benefits in terms of efficiency; but also, it may allow the operation of this train at much severe wind conditions.

The justification to why a train speed increase leads to a reduction on the impact of the considered geometry modifications, can be easily explained by how the considered yaw angle is computed. The yaw angle is computed as a vectorial summation of the train speed and the wind speed (see Fig. 18). As it can be gathered from Fig. 18, this means that increasing the train speed for a given wind speed/angle will involve a reduction of the relative yaw angle. As it can be observed in Fig. 12, the major differences in terms of aerodynamic loads occur for yaw angles above 30°. As previously described, increasing the speed of the train involves decreasing the relative yaw angle and thus, going under the aforementioned 30°, where the influence of the vehicle modifications is

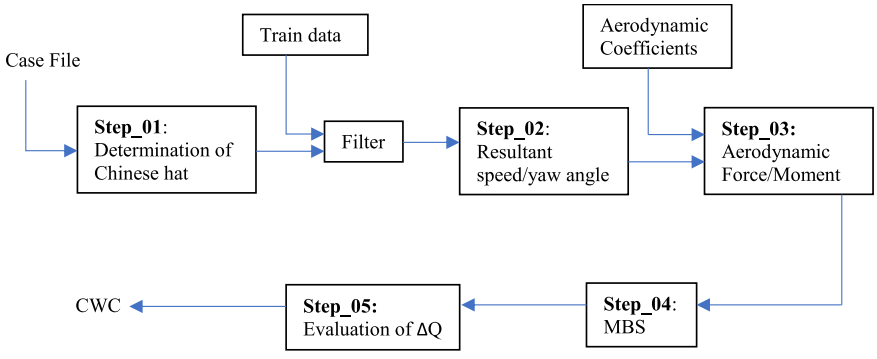

Fig. 16. Flow chart of CWC evaluation.

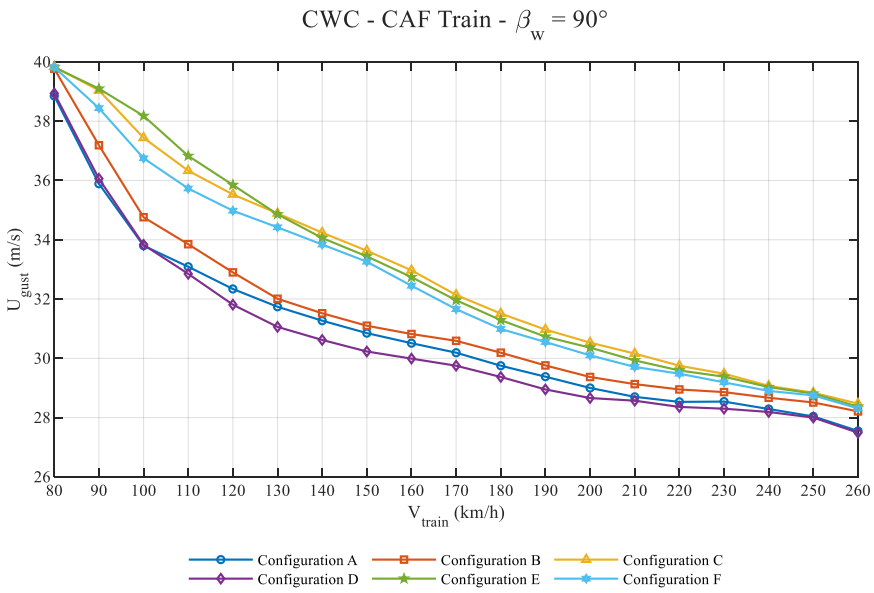

Fig. 17. Characteristic wind curve of the first vehicle, tangent track, wind angle $\beta_w = 90°$. Configurations A to F.

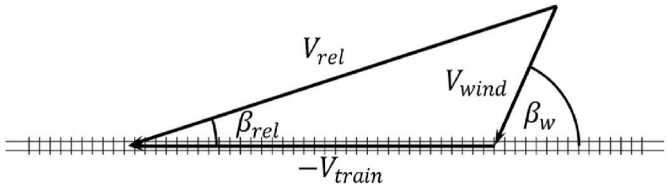

Fig. 18. Speed vector diagram.

lower. To illustrate the previous statement, a train running at 200 km/h with wind blowing at 30 m/s perpendicular to the track results in a yaw angle of 28°.

The results for configuration G, H, I, J and K, plus the baseline configuration A in terms of CWC are reported in Fig. 19. When the effects of the configurations affecting only the second car are analysed, it can be noticed that the closed roof leads to an almost constant increment along the whole range of speeds. The value of this increment is near 2 m/s for configuration J, with empty underbody, and it is close to 1.5 m/s when the underbody has some equipment.

It is interesting to note from the results of the multibody simulations that the critical bogie corresponds to the shared bogie between first and second car.

5. Conclusions

An experimental campaign has been performed to study the cross-wind stability of a conventional train. Aerodynamic coefficients have been measured by means of wind tunnel test on scaled models for different roof and underbody configurations of the first and second vehicles of the trainset.

Then, the correspondent CWC has been calculated for each train

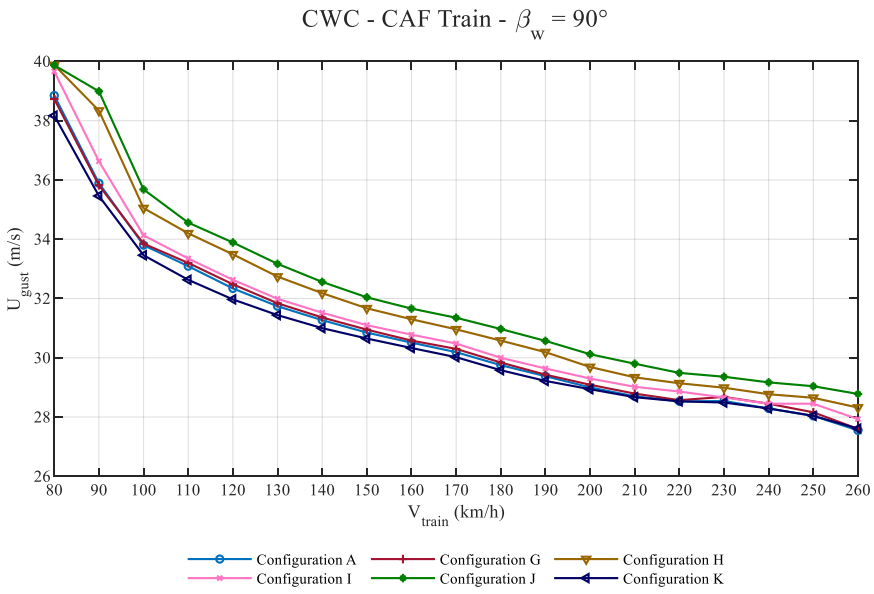

Fig. 19. Characteristic wind curve of the second vehicle, tangent track, wind angle $\beta_w = 90°$. Configurations A and G to K.

configuration using the procedure defined in the European Standard.

The principal findings are.

- Roof: Modifications on roof geometry have a significant effect on the crosswind sensitivity of the first and the second car. The effect of roof modifications has been observed to be dominant over the applied underbody modifications on the studied geometry. Having a completely covered roof usually leads to a significative reduction of aerodynamic coefficients, except lift, from 20° onwards. However, the lift increase is not able to compensate for the decrease on the lateral force and roll moment coefficients, resulting in an overall reduction of $C_{Mx,lee}$.
- Underbody: the analysed underbody designs do not have a significant influence due to the presence of lateral fenders that define the flow detachment point. For the first car, a smooth underbody seems to have a slight detrimental effect whereas for the second car, the clear underbody shows a slight improvement.
- The obtained CWCs are consistent with the results of the aerodynamic coefficients. The main influence of the applied geometry modifications tends to be concentrated between 40° and 60° angles according to Figs. 9 to 15. Thus, their influence would be dominant on trains speeds where these yaw angles are important (usually towards the lower range). For the first car an improvement of up to 4 m/s has been achieved with a completely covered roof (configuration E). Similarly, an improvement of up to 2 m/s has been observed for the second car when the roof is completely covered (configuration J). As train speed increases, the yaw angles to be considered are lower and therefore, the impact of geometry modifications is lower. This can be observed on the CWCs of Figs. 17 and 19.

CRediT authorship contribution statement

Carlos Esteban Araya Reyes: Conceptualization, Methodology, Formal analysis, Investigation, Writing – original draft. **Daniele Rocchi:** Resources, Supervision. **Gisella Tomasini:** Writing – review & editing, Supervision. **Mikel Iraeta Sánchez:** Writing - Review, Supervision. **Maialen Artano:** Software, Writing - Review.

Declaration of competing interest

The authors declare that they have no known competing financial interests or personal relationships that could have appeared to influence the work reported in this paper.

Data availability

The authors do not have permission to share data.

References

Araya Reyes, C.E., Baratelli, E., Rocchi, D., Tomasini, G., Iraeta Sánchez, M., Artano, M., 2022. Aerodynamic effects of different car body configurations in a conventional train under crosswinds. In: The Fifth International Conference on Railway Technology: Research, Development and Maintenance (Railways 2022). Montpellier. https://doi.org/10.4203/ccc.1.18.2.

Araya Reyes, C.E., Brambilla, E., Tomasini, G., 2023a. Evaluation of the aerodynamic effect of a smooth rounded roof on crosswind stability of a train by wind tunnel tests. Appl. Sci. 13, 232. https://doi.org/10.3390/app13010232.

Araya Reyes, C.E., Tomasini, G., Rocchi, D., 2023b. Crosswind assessment of conventional trains. In: 16th ICWE International Conference on Wind Engineering (ICWE 2023). Florence.

Baker, C.J., 1991a. Ground vehicles in high cross winds part I: steady aerodynamic forces. J. Fluid Struct. 5, 69–90. https://doi.org/10.1016/0889-9746(91)80012-3.

Baker, C.J., 1991b. Ground vehicles in high cross winds part II: unsteady aerodynamic forces. J. Fluid Struct. 5, 91–111. https://doi.org/10.1016/0889-9746(91)80013-4.

Baker, C.J., 1991c. Ground vehicles in high cross winds part III: the interaction of aerodynamic forces and the vehicle system. J. Fluid Struct. 5, 221–241. https://doi.org/10.1016/0889-9746(91)90478-8.

Bocciolone, M., Cheli, F., Corradi, R., Muggiasca, S., Tomasini, G., 2008. Crosswind action on rail vehicles: wind tunnel experimental analyses. J. Wind Eng. Ind. Aerod. 96, 584–610. https://doi.org/10.1016/j.jweia.2008.02.030.

Cheli, F., Ripamonti, F., Rocchi, D., Tomasini, G., 2010. Aerodynamic behaviour investigation of the new EMUV250 train to cross wind. J. Wind Eng. Ind. Aerod. 98, 189–201. https://doi.org/10.1016/j.jweia.2009.10.015.

Chen, Z., Liu, T., Jiang, Z., Guo, Z., Zhang, J., 2018. Comparative analysis of the effect of different nose lengths on train aerodynamic performance under crosswind. J. Fluid Struct. 78, 69–85. https://doi.org/10.1016/j.jfluidstructs.2017.12.016.

Diedrichs, B., 2010. Aerodynamic crosswind stability of a regional train model. Proc. Inst. Mech. Eng. F J. Rail Rapid Transit 224, 580–591. https://doi.org/10.1243/09544097JRRT346.

EN14067-6, 2018. Railway Applications - Aerodynamics, Part 6: Requirements and Test Procedures for Cross Wind Assessment, EN14067-6.

Giappino, S., Rocchi, D., Schito, P., Tomasini, G., 2016. Cross wind and rollover risk on lightweight railway vehicles. J. Wind Eng. Ind. Aerod. 153, 106–112. https://doi.org/10.1016/j.jweia.2016.03.013.

Guo, Z., Liu, T., Chen, Z., Xia, Y., Li, W., Li, L., 2020. Aerodynamic influences of bogie's geometric complexity on high-speed trains under crosswind. J. Wind Eng. Ind. Aerod. 196, 104053 https://doi.org/10.1016/j.jweia.2019.104053.

Hemida, H., Krajnović, S., 2009. Exploring flow structures around a simplified ICE2 train subjected to A 30° side wind using LES. Eng. Appl. Comput. Fluid Mech. 3, 28–41. https://doi.org/10.1080/19942060.2009.11015252.

Hemida, H., Krajnović, S., 2010. LES study of the influence of the nose shape and yaw angles on flow structures around trains. J. Wind Eng. Ind. Aerod. 98, 34–46. https://doi.org/10.1016/j.jweia.2009.08.012.

Liu, D., Wang, T., Liang, X., Meng, S., Zhong, M., Lu, Z., 2020. High-speed train overturning safety under varying wind speed conditions. J. Wind Eng. Ind. Aerod. 198, 104111 https://doi.org/10.1016/j.jweia.2020.104111.

Liu, D., Liang, X., Zhou, W., Zhang, L., Lu, Z., Zhong, M., 2022. Contributions of bogie aerodynamic loads to the crosswind safety of a high-speed train. J. Wind Eng. Ind. Aerod. 228, 105082 https://doi.org/10.1016/j.jweia.2022.105082.

Muñoz-Paniagua, J., García, J., 2019. Aerodynamic surrogate-based optimization of the nose shape of a high-speed train for crosswind and passing-by scenarios. J. Wind Eng. Ind. Aerod. 184, 139–152. https://doi.org/10.1016/j.jweia.2018.11.014.

Paradot, N., Grégoire, R., Stiepel, M., Blanco, A., Sima, M., Deeg, P., Schroeder-Bodenstein, K., Johnson, T., Zanetti, G., 2015. Crosswind sensitivity assessment of a representative Europe-wide range of conventional vehicles. Proc. Inst. Mech. Eng. F J. Rail Rapid Transit 229, 594–624. https://doi.org/10.1177/0954409715585368.

Resusta, Villalmanzo, Johnson, T., Paradot, N., 2018. Train Track Interaction Sector - Aerodynamics. UIC-ETF [white paper].

RSSB, 2013. The AeroTRAIN EU Project Summary Report.

Shuanbao, Y., Dilong, G., Zhenxu, S., Guowei, Y., Dawei, C., 2014. Optimization design for aerodynamic elements of high speed trains. Comput. Fluids 95, 56–73. https://doi.org/10.1016/j.compfluid.2014.02.018.

Sicot, C., Deliancourt, F., Boree, J., Aguinaga, S., Bouchet, J.P., 2018. Representativeness of geometrical details during wind tunnel tests. Application to train aerodynamics in crosswind conditions. J. Wind Eng. Ind. Aerod. 177, 186–196. https://doi.org/10.1016/j.jweia.2018.01.040.

Tomasini, G., Cheli, F., 2013. Admittance function to evaluate aerodynamic loads on vehicles: experimental data and numerical model. J. Fluid Struct. 38, 92–106. https://doi.org/10.1016/j.jfluidstructs.2012.12.009.

TSI, 2014. Technical specification for interoperability relating to the 'rolling stock–locomotives and passenger rolling stock' subsystem of the rail system in the entire European Union. Off. J. Eur. Union L 356, 228–393.

UIC, 2021a. SAFIRST - Assessment of Wind Exposure of the Line - Technical Report.

UIC, 2021b. SAFIRST - Application of Reference Characteristic Wind Curves - Technical Report.

UIC, 2021c. SAFIRST - Vehicle Assessment - Technical Report.

Wang, S., Wang, R., Xia, Y., Sun, Z., You, L., Zhang, J., 2021. Multi-objective aerodynamic optimization of high-speed train heads based on the PDE parametric modeling. Struct. Multidiscip. Optim. 64, 1285–1304. https://doi.org/10.1007/s00158-021-02916-0.

Xia, Y., Liu, T., Li, W., Dong, X., Chen, Z., Guo, Z., 2021. Numerical comparisons of the aerodynamic performances of wind-tunnel train models with different inter-carriage gap spacings under crosswind. J. Wind Eng. Ind. Aerod. 214, 104680 https://doi.org/10.1016/j.jweia.2021.104680.

Zhang, L., Zhang, J., Li, T., Zhang, Y., 2018. A multiobjective aerodynamic optimization design of a high-speed train head under crosswinds. Proc. Inst. Mech. Eng. F J. Rail Rapid Transit 232, 895–912. https://doi.org/10.1177/0954409717701784.